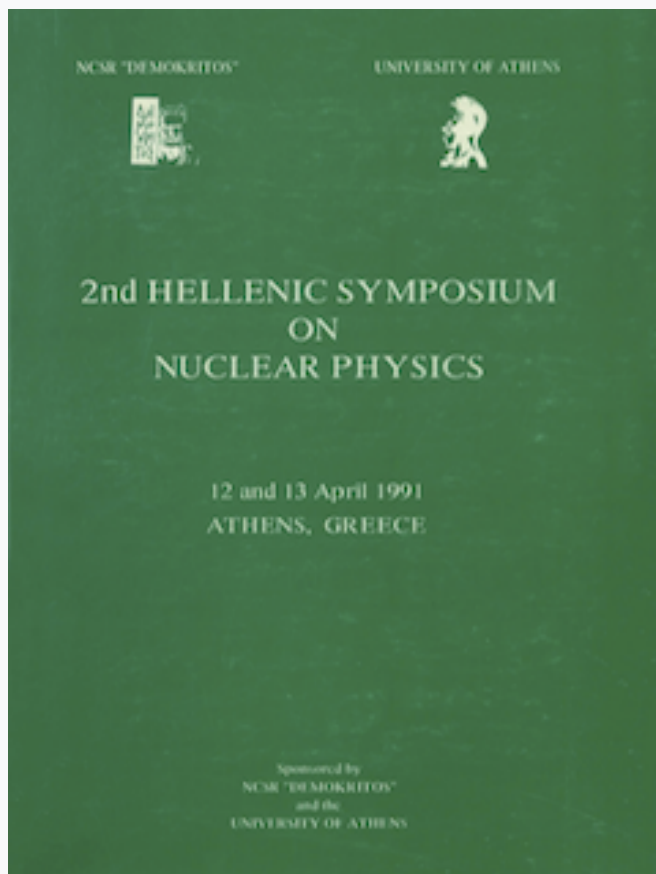


## HNPS Advances in Nuclear Physics

Vol 2 (1991)

HNPS1991



### LIFETIMES OF TRANSITIONAL NUCLEI IN THE A~130 REGION

*S. Harissopulos, A. Dewald, K. O. Zell, A. Gelberg, P. von Brentano*

doi: [10.12681/hnps.2858](https://doi.org/10.12681/hnps.2858)

#### To cite this article:

Harissopulos, S., Dewald, A., Zell, K. O., Gelberg, A., & von Brentano, P. (2020). LIFETIMES OF TRANSITIONAL NUCLEI IN THE A~130 REGION. *HNPS Advances in Nuclear Physics*, 2, 308–324. <https://doi.org/10.12681/hnps.2858>

## LIFETIMES OF TRANSITIONAL NUCLEI IN THE $A \approx 130$ REGION <sup>1</sup>

S. HARISSOPULOS

Institute of Nuclear Physics, N.C.S.R. "Demokritos"

GR-15310 Aghia Paraskevi, Attiki, Greece

A. DEWALD, K.O. ZELL, A. GELBERG, P. von BRENTANO  
Institute für Kernphysik, Universität zu Köln, D-5000 Köln, FRG

### Abstract

Mean lifetimes and side feeding times were measured for the  $8_1^+$  and  $10_1^+$  states of the nucleus  $^{120}\text{Xe}$  by using the Recoil Distance Doppler-Shift method (*RDDS*) and taking not only  $\gamma$ -singles spectra but also  $\gamma\gamma$ -coincidences. It was found that the side feeding times  $\tau^{sf}$  of these levels lie close to the effective lifetimes  $\tau^e$  of their precursors, i.e.  $\tau_{8_1^+}^{sf} \approx \tau_{10_1^+}^e$  and  $\tau_{10_1^+}^{sf} \approx \tau_{12_1^+}^e$ . Mean lifetimes for the ground state band members of the nuclei  $^{128}\text{Ba}$ ,  $^{130}\text{Ba}$ , and  $^{130}\text{Ce}$  were further determined by assuming either that the side feeding has the same time distribution as the discrete feeding or that the side feeding time  $\tau^{sf}$  is negligible, i.e.  $\tau^{sf} = 0$ . For these nuclei *RDDS* measurements were carried out without taking  $\gamma\gamma$ -coincidence spectra but only  $\gamma$ -singles spectra. The resulting  $B(E2)$  values, which were found to depend strongly on the assumed side feeding times, are compared with theoretical predictions.

### 1. Introduction

Lifetime measurements of excited nuclear states have been carried out for a long time. The aim of most of these measurements is the determination of the reduced transition probabilities  $B(L)$  of the  $\gamma$ -transitions deexciting the states of interest. The  $B(L)$  values can be easily obtained from the experiment using the following equation:

$$\frac{1}{\tau} = \frac{1}{\hbar} \cdot \frac{8\pi(L+1)}{L[(2L+1)!!]} \cdot \left(\frac{E_\gamma}{\hbar \cdot c}\right)^{2L+1} \cdot B(L) \quad (1)$$

where:

- $\tau$  is the experimentally determined lifetime,

---

<sup>1</sup>Presented by S. Harissopulos

- $L$  is the multipolarity of the  $\gamma$  -transition,
- $E_\gamma$  is the energy of the  $\gamma$  -ray,
- $\hbar$  is Planck's constant, and
- $c$  is the light velocity.

Reduced transition probabilities can be computed on the other hand in the framework of particular nuclear models, such as the shell model or some collective models (e.g. the rigid rotor or the Interacting Boson Model (IBM)) using the general equation:

$$B(L) = (2J_i + 1)^{-1} \cdot |\langle \Psi_f || M(L) || \Psi_i \rangle|^2 \quad (2)$$

where:

- $J_i$  is the spin of the initial state
- $\Psi_i$  is the wave function of the initial state,
- $\Psi_f$  is the wave function of the final state, and
- $M(L)$  is the operator of the electromagnetic interaction.

Hence, by comparing the experimentally derived  $B(L)$  values with those predicted by a certain model, one performs a very sensitive test of the wave functions used and obtains important information about the structure of the nuclear states of interest.

In order to obtain  $\tau$  experimentally one has to choose between different methods. Hereby, the crucial point is the order of magnitude of  $\tau$  to be determined. In the  $\gamma$  -spectroscopy one is usually interested in lifetimes down to some hundreds of  $fs$ . For  $\tau \geq 1 ns$  standard electronic techniques, like these described in ref.<sup>1)</sup>, are widely used, whereas for  $\tau \leq 1 ns$  the Doppler Shift techniques, i.e. the Recoil Distance Doppler Shift method (*RDDS*) and the Doppler Shift Attenuation Method (*DSAM*) have become the standard tools for measuring  $\tau$ . The former method (*RDDS*) is used to measure  $\tau$  in the range  $1 ps \leq \tau \leq 1 ns$ , whereas the latter technique (*DSAM*) is the most appropriate method to determine  $\tau \leq 1 ps$ .

The lifetimes reported here have been determined by carrying out *RDDS* experiments. Hence only the *RDDS* method will be here further presented. Details on the other methods mentioned above as well as on many other techniques used to measure lifetimes "indirectly" (such as the Coulomb excitation method or the resonance fluorescence) can be found in standard review articles <sup>2,3,4)</sup>.

## 2. The Recoil Distance Doppler Shift Method (*RDDS*)

### 2.1 THE BASIC PRINCIPLE

The basic principle of the *RDDS* method is illustrated in fig. 1. A very thin ( $\approx 0.5\text{mg/cm}^2$ ) target backed with a thicker foil (*backing*) is placed vertically to a HI-beam. In addition a very thick foil (*stopper*) is placed parallel to the target at a distance  $d$ .

The excited nuclei produced after a compound reaction in the target recoil freely into vacuum with a recoil velocity  $v$ . Part of these nuclei will decay in flight giving rise to a Doppler shifted peak in the  $\gamma$ -ray spectrum. The rest of the nuclei will arrive in the thick stopper and will decay there at rest, giving rise to another peak in the spectrum, which however is not Doppler shifted. Thus, for each  $\gamma$ -transition one obtains a Doppler unshifted peak (*stoppeak*) with an energy  $E_0$  equal to the energy difference of the initial and final state and additionally a broadened Doppler shifted peak (*flightpeak*) with an energy  $E_\gamma$  given by the following equation:

$$E_\gamma = E_0 \cdot \left(1 + \frac{v}{c} \cdot \cos\theta\right) \quad (3)$$

where  $\theta$  is the detection angle with respect to the beam axis.

As shown in fig. 1, the widths of the stoppeak and flightpeak corresponding to the same transition are different. The width of the stoppeak depends on the energy resolution of the Ge-detector used, whereas the width of the flightpeak depends additionally on the thickness of the target as well as on the finite solid angle subtended by the  $\gamma$ -ray detector.

The intensity  $N_s$  of the stoppeak can be expressed as

$$N_s = N_0 \cdot e^{-d/v\tau}, \quad (4)$$

whereas the intensity  $N_f$  of the flightpeak is given by the following equation

$$N_f = N_0 \cdot \left(1 - e^{-d/v\tau}\right) \quad (5)$$

where:

- $N_0$  is the total number of nuclei decaying from a particular level,
- $\tau$  is the lifetime of the level,
- $d$  is the distance between target and stopper, and
- $v$  is the recoil velocity of the residual nuclei.

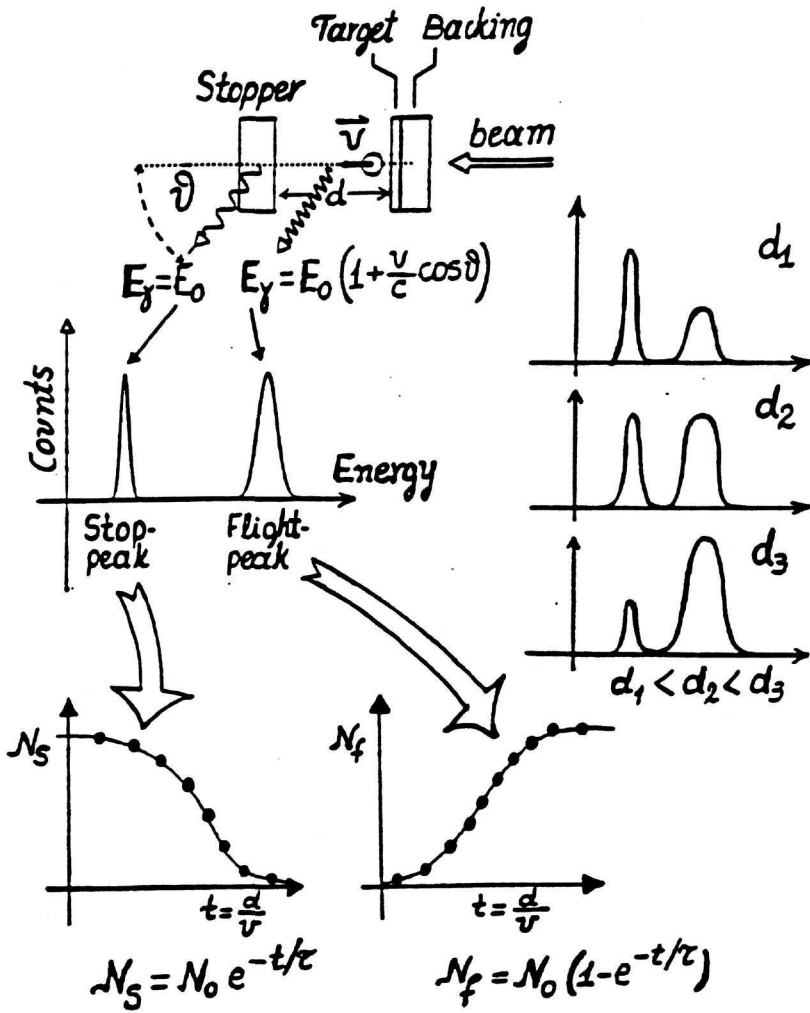


Fig. 1: The basic principle of the RDDS-method

By measuring  $N_s$  and/or  $N_f$  at different recoil distances  $d$ , an experimental decay curve can be obtained for the level of interest: As shown in fig. 1, by increasing  $d$ , the intensity  $N_s$  decreases whereas  $N_f$  increases. By fitting the function given by eq. (4) or eq. (5) to the experimental points determined for  $N_s$  or  $N_f$  respectively, the lifetime  $\tau$  can be derived.

## 2.2 DATA ANALYSIS AND SIDE FEEDING

In compound nucleus reactions the residual nuclei deexcite mainly by  $\gamma$ -cascades so that the simple eqs. (4) and (5) are no longer valid for states which are fed from other higher lying levels. The necessary corrections due to this feeding lead to a rather complicated expression for  $N_s$ , given by the following equation:

$$N_s(t) = P_1 \cdot e^{-t/\tau_1} + \sum_{j=2}^{j_{max}} M_{j1} \left( \frac{\tau_j}{\tau_1} e^{-t/\tau_j} - e^{-t/\tau_1} \right) \quad (6)$$

In this equation the level of interest is labeled with the subscript 1, whereas the subscript  $j = 2, 3, \dots, j_{max}$  runs for all states feeding level 1. Thus  $\tau_1$  is the lifetime of the level of interest,  $\tau_j$  the lifetime of the  $j$ -th state feeding level 1 and  $P_1$  is the direct population of level 1 by the neutron evaporation.  $M_{j1}$  is given by the general equation

$$M_{lm} = \frac{\tau_m}{\tau_l - \tau_m} \left( b_{lm} P_l + \sum_{k=m+1}^{l-1} M_{lk} b_{lk} \frac{\tau_l}{\tau_k} - \sum_{k>l}^{l_{max}} M_{kl} b_{lm} \right) \quad (7)$$

where  $b_{lm}$  is the branching ratio of the  $\gamma$ -transition deexciting level  $l$  and feeding level  $m$ .

The above eqs. (6) and (7) show that in order to determine the lifetime of a level in a  $\gamma$ -cascade, the contribution of all transitions feeding this level to its decay curve has to be correctly assessed: in order to obtain  $\tau_1$  one has to have accurate information on all  $\tau_j$ 's,  $P_j$ 's and  $b_{lm}$ 's.

The necessary values for  $P_j$  and the branching ratios  $b_{lm}$  are obtainable from an independent "intensity" measurement. Hereby, the intensities of all  $\gamma$ -transitions deexciting levels of the nucleus considered are measured by means of a thick target and at least one  $\gamma$ -ray detector placed at  $55^\circ$  to the beam axis.

In such a measurement, however, one often finds that the difference of the population of a given state, i.e the sum of the intensities of all  $\gamma$ -transitions feeding this state, from its depopulation is not zero. This intensity difference, which is called *side feeding* is the feeding from unobserved discrete or continuum  $\gamma$ -transitions.

In eq. (6) the side feeding of level 1 is represented by the direct population  $P_1$ , which is assumed to be prompt. However, if this is not real, i.e. the side feeding gives rise to a "side feeding time" comparable to the mean lifetime of the level of interest, then one has to a) eliminate the first term of eq. (6) and b) add to  $j_{max}$  the (unknown!) number of the side feeding transitions (*side feeders*). According to these, the data analysis becomes rather difficult by assuming that the side feeding time is not negligible: One needs a  $\tau_j$  (see eqs. 6 and 7), i.e. a decay curve, for each side feeder, which, however, is very weak and therefore "hidden" in the background of the spectra. Consequently, the contribution of side feeding on the decay curve of the level of interest can, in contrast to the feeding from discrete levels (*discrete feeding*), not be assessed: For the discrete levels feeding the state of interest one can obtain their lifetimes from their decay curves, which can be obtained experimentally. Hence, by fitting eq. (6) to the experimental points of  $N_s$ , in order to obtain the lifetime of the level of interest, one has more than one unknown (free) parameters, namely the lifetime  $\tau_1$  as well as all the  $\tau_j$ 's associated with the side feeding transitions.

In a number of experimental investigations<sup>5,6,7</sup>) it was assumed that the side feeding is prompt. In other works<sup>8,9</sup>), however, the contribution of side feeding to the decay curves of the levels of interest has been treated by means of an  $\chi^2$ -analysis: an arbitrary number of side feeders is assumed to fit the data by varying the respective intensities and feeding times.

In the present work, the data were first analysed by assuming that the side feeding is to be associated to *only one*  $\gamma$ -transition. Then, the side feeding time  $\tau^{sf}$  was varied over a wide range by fitting eq. (6) to the decay curves. This procedure, however, showed sizeable errors, in particular for short lived states with significant side feeding intensity, and an  $\chi^2$ -analysis of the decay curves gave in many cases ambiguous results for the lifetime as well as for the side feeding time. This is demonstrated in fig. 2, which shows the decay curve (solid circles) of the  $8_1^+$  state in  $^{128}\text{Ba}$ . The solid curve labeled with "a" was obtained assuming a prompt side feeding, i.e.  $\tau^{sf} = 0$ , and yields a lifetime of 3.3(6) ps with an  $\chi^2 = 1.2$ . In contrast, the solid curve labeled with "b" was obtained assuming  $\tau^{sf} = 4.3$  ps and gives a lifetime of 1.5(7) ps with an  $\chi^2 = 1.1$ . Curves "a" and "b" are almost identical, although rather different side feeding times have been hereby assumed to fit the data. As shown in table 1, the assumed side feeding time and the resulting lifetime of the  $8_1^+$  state are strongly correlated. Moreover, the resulting  $B(E2)$  values for the  $8_1^+ \rightarrow 6_1^+$  transition are rather different for different side feeding times.

Consequently, by comparing experimental  $B(E2)$  values of  $\gamma$ -transitions depopulating levels fed significantly from side feeders with  $B(E2)$ s predicted by a nuclear model, a correct assessment of the influence of the side feed-

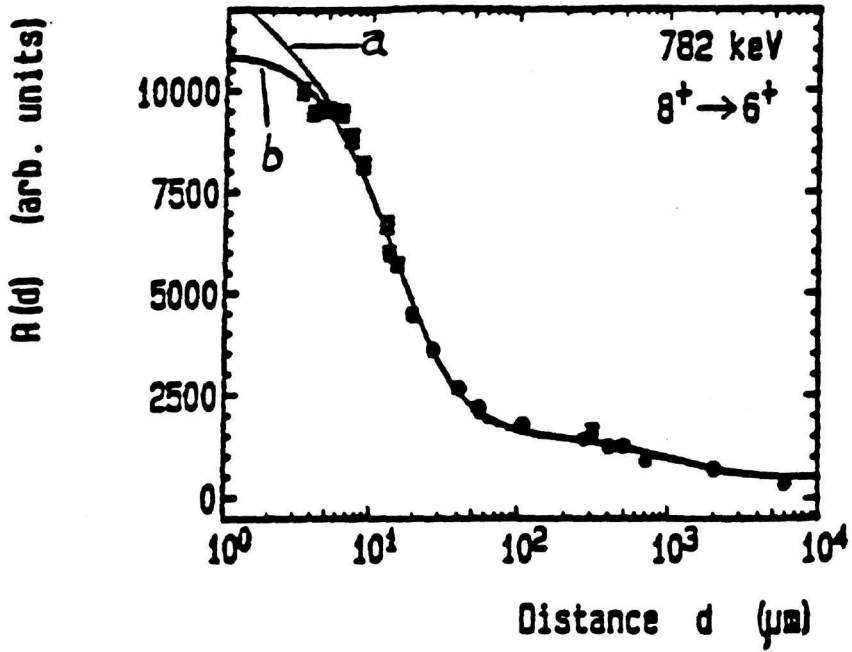


Fig. 2: Decay curve of the  $8_1^+$  state in  $^{128}\text{Ba}$ . Curve "a" was obtained assuming  $\tau^{sf} = 0$ , whereas curve "b" was derived assuming  $\tau^{sf} = 4.3$  ps.

Curve	$\chi^2$	$\tau^{sf}$ (ps)	$\tau$ (ps)	$B(E2; 8_1^+ \rightarrow 6_1^+)$ (W.u)
a	1.2	0	3.3(8)	22(6)
b	1.1	4.3	1.5(9)	48(7)

Table 1: Fit results for the  $8_1^+$  state in  $^{128}\text{Ba}$ .



ing times is particularly important. Due to these problems, the significant deviations from the rigid rotor values of  $B(E2)$ s observed<sup>5,9,10,11</sup>) below back-bending could be the result of a systematic error and not the "signature" of an unknown effect.

In order to avoid these problems it is necessary to eliminate the side feeding by carrying out *RDDS* measurements in combination with  $\gamma\gamma$  - coincidences. Then lifetimes can be measured independently, i.e without any assumption on the side feeding times. This was the next step in the present work.

### 3. Experiments and results

As mentioned above, the aim of our lifetime measurement, carried out in combination with  $\gamma\gamma$ -coincidences, was to obtain lifetimes directly, without any assumption on side feeding, by eliminating it, and to further determine side feeding times. For this purpose, it was necessary to choose excited states in a nucleus which were fed significantly from side feeders.

From previous  $\gamma$  -measurements<sup>12)</sup> it was known that the  $8_1^+$  and  $10_1^+$  states of  $^{120}\text{Xe}$  produced with the  $(^{13}\text{C},3n)$ -reaction at a beam energy of 54.5 MeV, were populated by a large amount of side feeding (22.8% and 48.4% respectively). In the present measurement carried out in  $^{120}\text{Xe}$ , four Ge-detectors, as shown in fig. 3, were used. Three of them were placed at  $90^\circ$  with respect to the beam and the rest one detector was positioned at  $0^\circ$  to the beam. More experimental details are given in ref. <sup>13)</sup>.

$\gamma\gamma$  -coincidences between each detector at  $90^\circ$  and the detector at  $0^\circ$  were recorded at different distances  $d$  between target and stopper and sorted off-line onto matrices. By setting energy gates on the  $90^\circ$  detectors, where no Doppler-shifted peaks occur, we obtained from the  $0^\circ$  detector  $\gamma$  -spectra in coincidence with  $\gamma$  -transitions of the ground band up to the  $12_1^+ \rightarrow 10_1^+$ . By carrying out this procedure at each recoil distance  $d$ , where spectra were taken, we obtained decay curves in coincidence with these  $\gamma$  -transitions. The important point in the analysis is that by setting an energy gate on the transition  $12_1^+ \rightarrow 10_1^+$ , the  $10_1^+$  state is populated only through this  $\gamma$  -transition, i.e the side feeding is eliminated and the decay curve obtained in this way is not influenced by it. The lifetime obtained from the fit to this decay curve, which is shown in fig. 4, is the "true" lifetime of the  $10_1^+$  state, since no assumption on the side feeding time was necessary. On the other hand, the side feeding of the  $10_1^+$  state contributes to all decay curves of this level, which were taken in coincidence with a  $\gamma$  -transition below the  $8_1^+$  state. By assuming further that the side feeding is to be associated with only one "effective" transition and using the "true" lifetime obtained as described

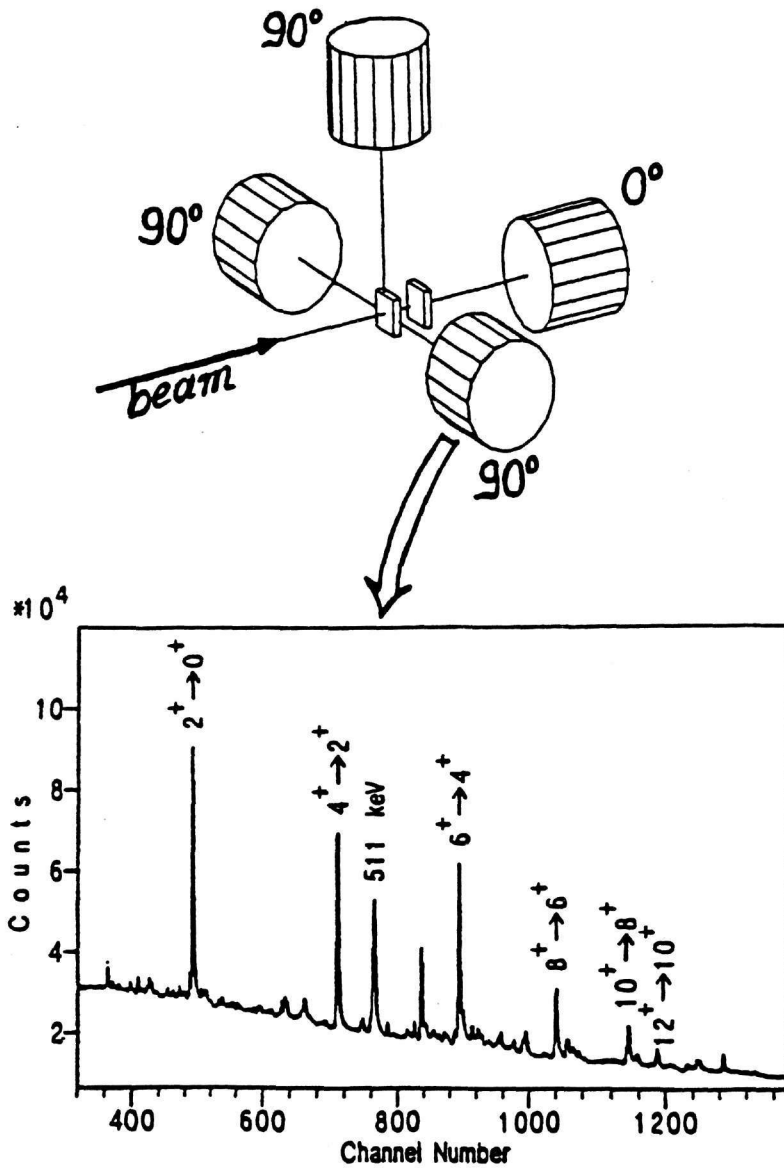


Fig. 3: RDDS-measurement in  $^{120}\text{Xe}$  in combination with  $\gamma\gamma$ -coincidences. The spectrum shown is a spectrum taken with a  $90^\circ$  detector with completely open energy gate

above, one can extract an "effective" side feeding time for the  $10_1^+$  state: by fitting eq. (6) to such a decay curve only one lifetime is unknown, namely the effective side feeding time  $\tau^{sf}$ . In fig. 5 the decay curve of the  $10_1^+$  state obtained from  $\gamma$ -singles (solid circles) as well as the decay curve of this state taken in coincidence with all transitions below the  $8_1^+$  level (stars) are shown.

The above mentioned procedure was also carried out for the  $8_1^+$  state. The results of the data analysis are summarized in table 2. From this table a very important feature of side feeding is to be seen: The effective side

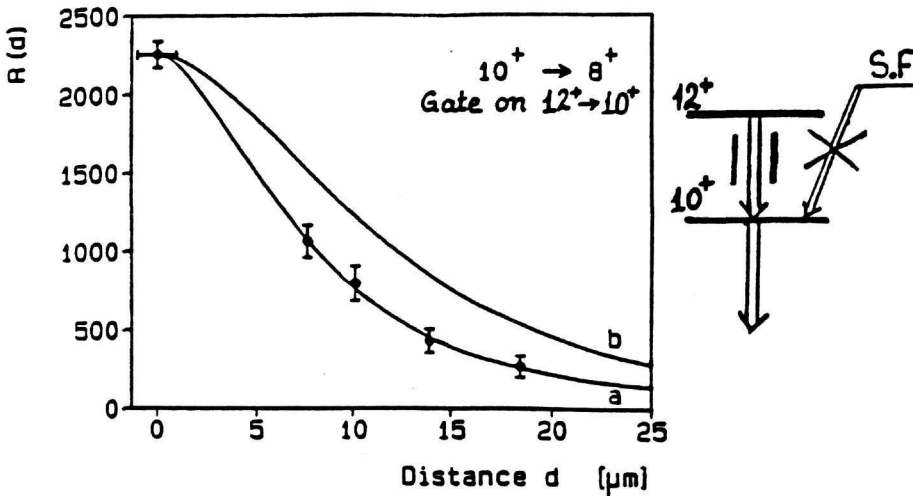


Fig. 4: Decay curve of the  $10_1^+$  state in  $^{120}\text{Xe}$ . Curve "a" is the fit from which the true lifetime of the level was derived, whereas curve "b" represents expected coincidence rates assuming a prompt side feeding, i.e.  $\tau^{sf} = 0$

feeding times obtained for the levels considered lie very close to the effective lifetimes of their precursors. (Compare the effective lifetime of e.g. the  $12_1^+$  state and the effective side feeding time of the  $10_1^+$  state).

This experimental fact, which is further supported by other experimental works<sup>14)</sup> in different mass regions, was further taken into account in order to analyse data of *RDDS* experiments in which only  $\gamma$ -singles and not  $\gamma\gamma$ -coincidence spectra were measured. Such measurements were carried out in Cologne for the nuclei  $^{128}\text{Ba}$ ,  $^{130}\text{Ba}$  and  $^{130}\text{Ce}$ . The reactions used to

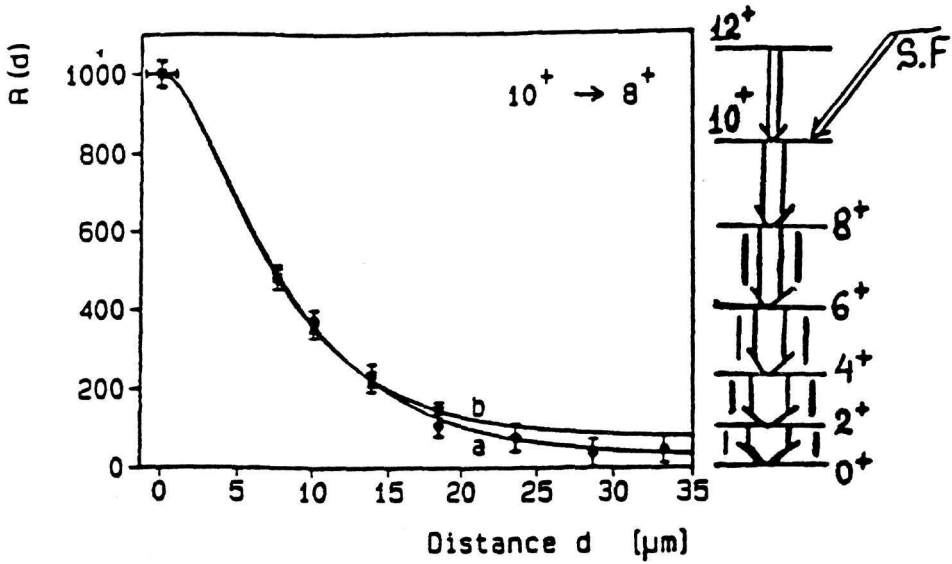


Fig.5: Decay curves of the  $10_1^+$  state of  $^{120}\text{Xe}$ . With solid circles is indicated the decay curve obtained from  $\gamma$ -singles spectra, whereas stars indicate the decay curve taken in coincidence with all transitions below the  $8_1^+$  state. The solid curves "a" and "b" are the respective fits from which the side feeding time was derived

Level (keV)	$I^\pi$ ( $\hbar$ )	side feeding intensity (%)	lifetime $\tau$ (ps)	side feeding time $\tau^{sf}$ (ps)		effective lifetime $\tau^e$ (ps)	
				(a)	(b)	(a)	(b)
2099.1	$8^+$	22.8(26)	1.9(6)	3.5(26)	4.1(28)		
2872.6	$10^+$	48.4(32)	1.0(5)	2.2(13)	2.9(14)	3.8(4)	3.9(4)
3676.4	$12^+$					2.4(5)	1.8(4)

Table 2: Results of the RDDS-measurement with  $\gamma\gamma$ -coincidences in  $^{120}\text{Xe}$ . Effective lifetimes and side feeding times obtained from  $\gamma$ -coincidence spectra are given in columns labeled with (a), whereas these obtained from  $\gamma$ -singles spectra are given in columns labeled with (b).

produce these nuclei were  $^{118}\text{Sn}(^{13}\text{C},3\text{n})^{128}\text{Ba}$  at 53 MeV,  $^{120}\text{Sn}(^{13}\text{C},3\text{n})^{130}\text{Ba}$  at 55 MeV, and  $^{117}\text{Sn}(^{16}\text{O},3\text{n})^{130}\text{Ce}$  at 76 MeV. Experimental details for these measurements can be found in ref. <sup>15</sup>). The analysis of the data was carried out by means of a new method called the "Differential Decay Curve Method" (*DDCM*) proposed recently by *Dewald et al.*<sup>16</sup>). The main advantage of this method, which is presented in detail in ref. <sup>16</sup>) and will be therefore not presented here, is that systematic errors can be discovered much easier than in the conventional analysis, which is described in section 2.2. By using *DDCM* we assumed either that (I) side feeding has the same time distribution as the discrete feeding or (II) side feeding is prompt. In the former assumption the time distribution of side feeding  $N^{sf}(t)$  was obtained from the following eq. (8).

$$N^{sf}(t) = \eta \cdot \sum_j N_j^s(t) \quad (8)$$

where:

- $N_j^s(t)$  are the intensities of the stoppeaks of the  $\gamma$  -transitions feeding the level of interest. These intensities are corrected for the efficiency of the detectors used as well as for the  $\gamma$  -angular distribution of the respective  $\gamma$  -transitions.
- $\eta$  is the relative intensity difference obtained from the "intensity" measurement mentioned above in section 2.2

By assuming that side feeding is prompt one simply sets  $\eta=0$ , so that in the basic equation used in *DDCM* to obtain the lifetime of a particular level no side feeding term, i.e  $N^{sf}(t)$ , is included. The equations used by *DDCM* are given in ref.<sup>16</sup>). The mean lifetimes obtained for these nuclei by means of *DDCM* are summarized in table 3.

A very important feature of *DDCM* is that one can determine at each recoil distance  $d$ , where spectra were taken, a value for the lifetime of a particular level. These values clearly must lie on a straight line in absence of systematic errors. This was not the case for the lifetimes of table 3, which are given in square brackets.

The  $B(E2)$  values obtained for the above nuclei are compared with theoretical predictions in figs. 6 and 7.

Table 3: Mean lifetimes  $\tau$  determined using DDCM (see text) and assuming that: (I) the side feeding time is equal to the effective discrete feeding time, i.e.  $\tau_j^{sf} = \tau_{j+2}^e$ , and (II) the side feeding is prompt, i.e.  $\tau^{sf} = 0$ . Lifetimes given in square brackets are, according to the DDCM, affected by systematic errors. The relative side feeding intensity ( $F^{sf}$ ) of each level is given in the last column.

Level $J^\pi$	(I)	$\tau$ (ps)	(II)	$F^{sf}$ (%)
		$^{128}\text{Ba}$		
$2_1^+$	129(5)		129(5)	0
$4_1^+$	6.7(4)		[7.6(3)]	6.3(24)
$6_1^+$	1.2(3)		[2.2(2)]	10.3(22)
$8_1^+$	[1.1(3)]		[2.9(2)]	26.9(32)
$10_1^+$	0.7(5)		[2.5(4)]	32.9(64)
		$^{130}\text{Ba}$		
$2_1^+$	52(3)		54(3)	4.5(4)
$4_1^+$	6.0(4)		6.5(4)	4.5(4)
$6_1^+$	1.0(3)		2.2(3)	9.3(18)
$8_1^+$	0.5(3)		1.5(3)	21.7(30)
		$^{130}\text{Ce}$		
$4_1^+$	6.0(3)		7.0(2)	6.4(22)
$6_1^+$	0.9(3)		[2.4(2)]	7.7(12)
$8_1^+$	0.4(2)		[1.1(2)]	6(1)
$10_1^+$	0.6(2)		1.2(2)	8(2)

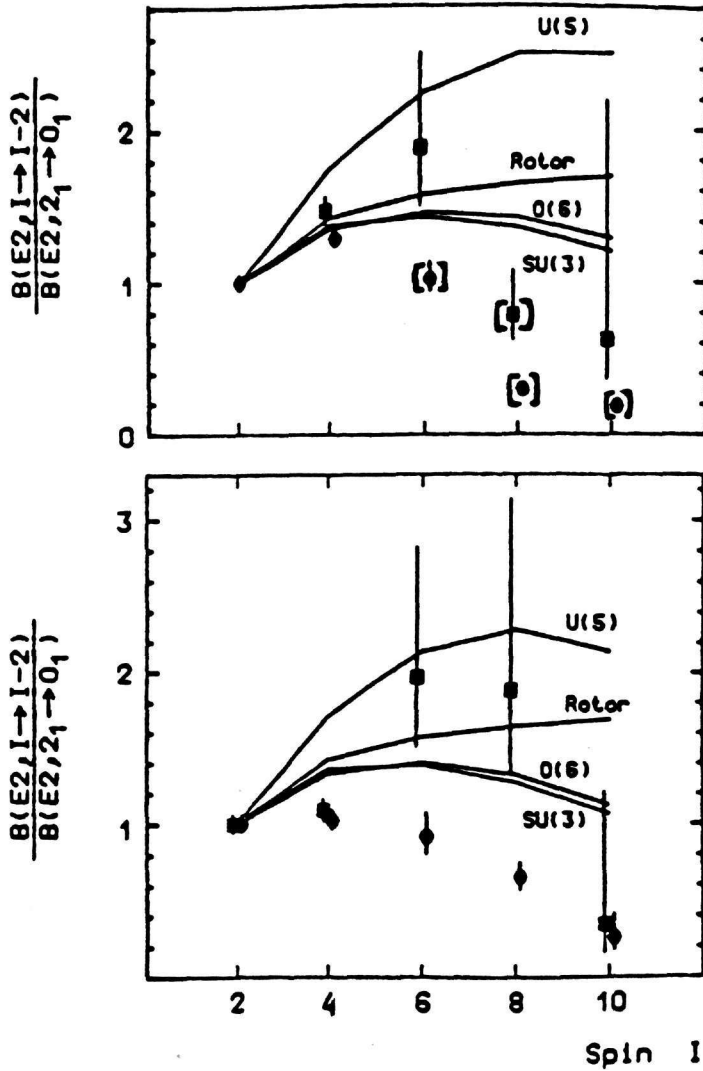


Fig. 6: Relative  $B(E2)$  values obtained for the ground state band of  $^{128}\text{Ba}$  (above) and  $^{130}\text{Ba}$  (below) assuming either that side feeding has the same time distribution as the discrete feeding (solid rectangles) or side feeding time is prompt (solid circles). Data points in squared brackets are affected by systematic errors. The solid curves indicate the predictions of the rigid rotor model and the three limits U(5), O(6) and SU(3) of the Interacting Boson Model (IBM-1).

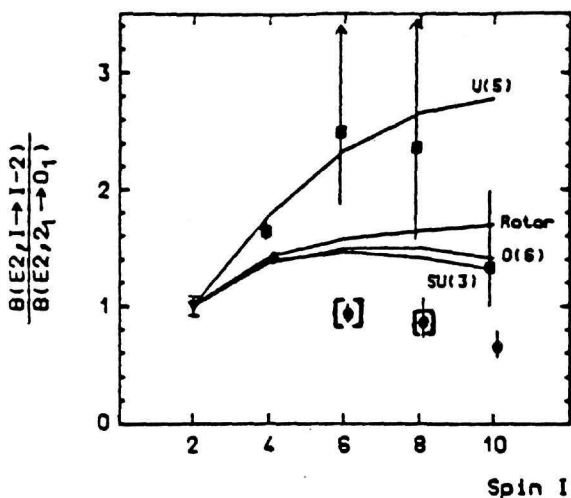


Fig. 7: Relative  $B(E2)$  values determined in the ground state band of  $^{130}\text{Ce}$ . For explanations see caption of fig. 6

#### 4. Conclusions

The strong dependence observed in the present work of the lifetimes of states with significant side feeding from the side feeding times suggests that in order to obtain reliable lifetimes the *RDDS*-measurements have to be carried out in combination with  $\gamma\gamma$ -coincidences. Only such measurements can provide us with both the "true" lifetime as well as the side feeding time of such a state.

The side feeding times measured for the  $8_1^+$  and  $10_1^+$  states of  $^{120}\text{Xe}$  show clearly that the side feeding is not prompt, i.e.  $\tau^{sf} \neq 0$ .

Side feeding times measured in  $^{120}\text{Xe}$  lie very close to the effective discrete feeding times. By assuming that side feeding has the same time distribution as the discrete feeding, reliable lifetimes were obtained in the present work for the nuclei  $^{128}\text{Ba}$ ,  $^{130}\text{Ba}$  and  $^{130}\text{Ce}$ . However, before generalizing such an assumption, more *RDDS*-measurements in combination with  $\gamma\gamma$ -coincidences have to be carried out.

Since many of the  $B(E2)$  values determined in the present work are strongly correlated with the side feeding time, the deviations from the rigid rotor values of  $B(E2)$  reported in some other nuclei below backbending could be attributed to the lack of accurate information of the respective side feeding times. The results of this work do not justify a  $B(E2)$ -anomaly effect in the investigated nuclei.



## References

- [1 ] K.E.G. Löbner, *Delayed coincidence methods in: The electromagnetic interaction in nuclear spectroscopy*, (W.D. Hamilton, ed.), p.173, North Holland Publishing Co.,1975.
- [2 ] P.J. Nolan, and J.F. Scharpey-Schafer, *The measurement of the lifetimes of excited nuclear states*, Rep. Prog. Phys. 42(1979)1-86.
- [3 ] D.B. Fossan, and E.K. Warburton, *Lifetime Measurements in: Nuclear Spectroscopy and Reactions*, (J. Cerny, ed.), Part C, p. 307, Academic Press, New York, 1974.
- [4 ] T.K. Alexander, and J.S. Foster, *Lifetime measurements of excited nuclear levels by Doppler-Shift Methods*, Adv. Nucl. Phys. 10(1978)197-331.
- [5 ] P.J. Nolan, R. Aryaeinejad, D.J.G Love, A.H. Nelson, P.J. Smith, D.M. Todd, P.J. Twin, J.D. Garrett, G.B. Hagemann, and B. Herskind, *Electromagnetic transitions in  $^{130}\text{Ce}$* , Phys. Script. T5(1983)153.
- [6 ] A. Dewald, U. Kaup, W. Gast, A. Gelberg, H.-W. Schuh, K.O. Zell, and P. von Brentano, *High spin states of  $^{84}\text{Sr}$ .*, Phys. Rev. C25(1982)226-239.
- [7 ] J.C Wells, N.R. Johnsson, J. Hattula, M.P. Fewell, D.R. Haenni, I.Y. Lee, F.K. McCowan, J.W. Johnson, and L.L. Riedinger, *Evidence for collective behaviour in  $^{128}\text{Ce}$  from lifetime measurements*, Phys. Rev. C30(1984)1532-1537.
- [8 ] H. Emling, E. Grosse, R. Kulesa, D. Schwalm, and H.J. Wollersheim, *Rotation-Induced shape transitions in Dy Nuclei*, Nucl. Phys. A419(1984)187-220.
- [9 ] D. Husar, S.J. Mills, H. Gräf, U. Neumann, D. Pelte, and G. Seiler-Clark, *Lifetimes of the yrast states of even Ce isotopes*, Nucl. Phys. A292(1977)267-280.
- [10 ] G. Seiler-Clark, D. Husar, R. Novotny, H. Gräf, and D. Pelte, *Backbending and E2 reduction in  $^{126}\text{Ba}$* , Phys. Lett. 80B(1979)345-346.
- [11 ] H. Hanewinkel, W. Gast, U. Kaup, H. Harter, A. Dewald, A. Gelberg, R. Reinhardt, P. von Brentano, A. Zemel, C.E. Alonso, and J.M. Arias, *Pre-alignment B(E2)-anomaly in  $^{124}\text{Xe}$* , Phys. Lett. 133B(1983)9-12.
- [12 ] K. Loewenich, K.O. Zell, A. Dewald, W. Gast, A. Gelberg, W. Lieberz, P. von Brentano, and P. van Isacker, *In-beam spectroscopy of  $^{120}\text{Xe}$* , Nucl. Phys. A460(1986)361-372.
- [13 ] S. Harissopoulos, A. Dewald, A. Gelberg, P. von Brentano, K. Loewenich, K. Schiffer, and K.O. Zell, *Lifetime measurements in  $^{120}\text{Xe}$ , using a coincidence plunger technique*, Nucl. Phys. A467(1987)528-538.

- [14 ] F. Cristancho, K.P. Lieb, J. Heese, C.J. Gross, W. Fieber, Th. Osipowicz, S. Ulbig, K. Bharuth-Ram, S. Skoda, J. Eberth, A. Dewald, and P. von Brentano, *Side-feeding times and level lifetimes measured in the reaction  $^{54}\text{Fe}(^{32}\text{S},3p)^{83}\text{Y}^*$* , Nucl. Phys. **A501**(1989)118-136.
- [15 ] S. Harissopulos, *Lebensdauer der niedrigsten kollektiven Zustände in den Kernen  $^{120}\text{Xe}$ ,  $^{128}\text{Ba}$ ,  $^{130}\text{Ba}$ ,  $^{130}\text{Ce}$* , Ph. D. Thesis, Köln (1989), unpublished.
- [16 ] A. Dewald, S. Harissopulos, and P. von Brentano, *The Differential Plunger and the Differential Decay Curve Method for the Analysis of Recoil Distance Doppler-Shift Data*, Z. Phys. **A334**(1989)163-175.